International Journal of Automotive Technology, Vol. 7, No. 4, pp. 493–500 (2006)

1229-9138/2006/028-13

DISTRIBUTION OF FUEL MASS AFTER WALL IMPINGEMENT OF DIESEL SPRAY

K. N. KO[1)*], J. C. HUH[2)] and M. ARAI[3)]

[1)]Clean Energy Education Center, Cheju National University, Jeju 690-756, Korea
[2)]Department of Mechanical Engineering, Cheju National University, Jeju 690-756, Korea
[3)]Department of Mechanical System Engineering, Gunma University, Kiryu 376-8515, Japan

(Received 28 March 2005; Revised 16 March 2006)

ABSTRACT–Investigation on the fuel adhering on a wall was carried out experimentally to clarify the characteristics of impinging diesel sprays. Diesel sprays were injected into a high-pressure chamber of cold state and impinged to a wall having various impingement distances and ambient pressures. Photographs of both the fuel film and the post-impingement spray were taken through a transparent wall. Adhered fuel mass on a wall was measured by means of dividing into two types of fuel state: the fuel film itself; and sparsely adhered fuel droplets. Adhering fuel ratio was predicted and further the distribution of fuel mass for impinging diesel spray was analyzed as a function of time. As result, with an increase of the ambient pressure, both the maximum fuel film diameter and the adhered fuel ratio decreased. Based on some assumptions, the adhering fuel mass increased rapidly until the fuel film diameter approached the maximum value, and then increased comparatively gradually.

KEY WORDS : Diesel spray, Spray tip penetration, Spray tip velocity, Spray cone angle, Nozzle aspect ratio

1. INTRODUCTION

Because of the evident benefit of higher thermal efficiency than other engines, direct injection diesel engines have been used in various fields. Its utilization is now expanding to smaller engine fields. The smaller the cylinder bore of engine becomes, the shorter the distance between the injection nozzle tip and the piston cavity wall becomes. Accordingly it is inevitable that the fuel injected through the nozzle impinges to the piston cavity wall. The spray impingement forms a liquid film adhered on the piston and cylinder wall. This liquid film is evaporated by surroundings and the wall surface heated, and it results in an increase of smoke level. Gonzalez *et al.* (1991) reported that the accumulation of fuel on a cylinder wall led to an increase in smoke levels during cold start of engine. So when engine researchers design an engine, they should consider the effect of spray-wall impingement in the combustion chamber for an optimum design and lower emission levels.

It was found by several researchers (Matsuoka *et al.*, 1984; Takasaki *et al.*, 1994, etc) that ignitions of impinging sprays in test engines occurred after wall impingement. Zurlo and Chigier (1991) had taken pictures of the impinging sprays from underneath a plate under atmospheric conditions. They measured fuel droplet size, and reported that the impinging spray was mainly re-atomized by breakup of ligaments after the impingement. Senda *et al.* (1997) proposed a sub-model for a dispersion process of the impinging spray concerning fuel film formation process. The fuel film model that was incorporated with the interaction between spray-wall and spray-film was also proposed by Stanton and Rutland (1998). They formulated a fuel film mathematical model using a thin film assumption. Ko *et al.* (2001) pointed out that volume of post-impingement spray was larger than that of a free spray at the same inspection time, when the spray impinged to a wall before a break-up of it.

In order to optimize a spatial distribution of the spray in a combustion chamber of a small D.I. diesel engine, many investigators have suggested important behaviors of diesel sprays concerning to the spray impingement to a projection attached on a flat wall (Tsunemoto *et al.*, 1996), spray-to-jet (Chikahisa *et al.*, 2002), spray-to-spray (Amagai *et al.*, 2003) and so on. These behaviors might result in reduction of harmful emissions such as particulate matters and NOx from diesel engines. Koo (2003) had investigated the spray characteristics with changes of nozzle geometry and an operating pressure. Characteristics of spray issuing from common rail injector were studied by Park and Lee (2003). Using spray visualization system, phase Doppler particle analyzer (PDPA) and KH-DDB

*Corresponding author. e-mail: gnkor2@cheju.ac.kr

model, they compared experimental results with calculated results.

In the investigation reported here, fuel mass behavior of wall-impingement diesel spray was studied. Photographs of fuel films after wall impingements were taken with sprays impinging to a wall. A mass ratio of adhering fuel to total fuel injected was estimated as a function of elapsing time from injection start. Based on the adhering fuel mass with elapsing time, the distribution of fuel mass for the diesel spray impinging on a flat wall was analyzed by means of dividing into three parts; the spray part before impingement, the part of fuel adhering on the wall and the spray part after impingement.

2. EXPERIMENTAL APPARATUS AND PROCEDURE

The experimental apparatus is shown in Figure 1. It was composed of an injection system, a pressure vessel and a spray imaging system. In order to make a single injection, a single shot pulse generator, a solenoid valve and a dummy nozzle were used. A single-hole type diesel injection nozzle with a hole diameter of 0.24 mm and a length-to-hole diameter ratio of 2.5 was used. Valve opening pressure of the nozzle was 19.0 MPa and the maximum injection pressure was about 28.0 MPa. Diesel fuel (JIS No. 2) was used as an injection fuel. The injection pump was coupled to a DC motor and the pump speed was 600 rpm.

The pressure vessel was filled with nitrogen gas and the ambient pressure was set at 0.5 MPa, 1.0 MPa and 1.5 MPa at room temperature. The impingement distances from the nozzle tip to a wall were set at 10 mm, 30 mm and 50 mm. The wall distance, Lw of 30 mm corresponds to real condition of a high speed small DI diesel engine.

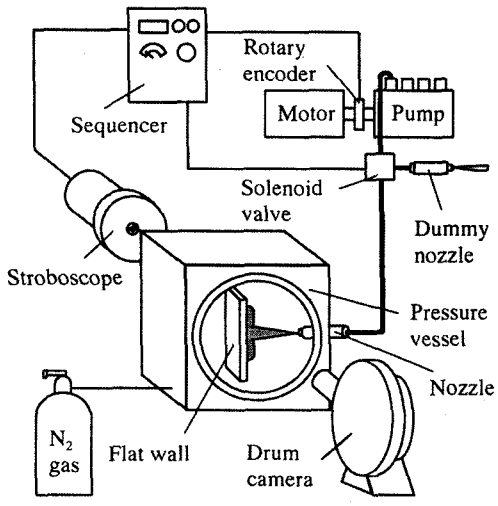

Figure 1. Experimental apparatus.

For the comparative study, we conducted the experiments at L_w = 10 mm and 50 mm. Injection rate was measured using a Bosch type injection rate meter. Injection period was 1.8 ms, and total injection quantity was 9.96 mg/st. Since fuel adhering might be influenced by affinity between fuel and wall material, aluminum material similar to the material of a piston of small engine was used as a wall. An aluminum circular plate with 95 mm diameter and 2 mm thickness was put on an impingement wall to catch the adhered fuel. In the case of taking photographs of the adhered fuel film, the transparent acrylic wall (150 mm × 40 mm, and thickness of 10 mm) was equipped into the pressure vessel. These two-type plates as the walls were set at vertical against the direction of spray axis.

The shape of the fuel film after impingement was taken with a 36 mm still camera, which was located at the rear of the transparent wall. Also, a stroboscope was set to observe the behavior of the diesel spray. The spray images were taken with a drum camera continuously at an interval of about 0.14 ms.

Figure 2 explains the measurement and estimation method of adhered fuel mass. The aluminum wall was set at perpendicular in order to minimize the re-attachment effect of splashed droplets after impingement. The real adhered fuel mass could be obtained with the following method. After the spray was impinged to the aluminum circular wall, the mass of the wall with adhered fuel was measured using a precision balance, whose sensitivity is 0.01 mg. And then, since the sparsely adhered fuel encircling with the fuel film could not be neglected, the adhered fuel mass on the wall was analyzed by means of dividing into two types; the fuel film itself and the sparsely adhered fuel droplets encircling with the film. However because of the gravity effect, the fuel film slid down along the wall. So, we wiped sparsely adhered droplets on the upper half area of the circular wall with a clean paper, and measured again the mass of the wall with adhered fuel remained on that. Taking twice of the mass of wiped fuel, we could obtain the value as the surrounding adhered droplets. Then, the fuel film mass

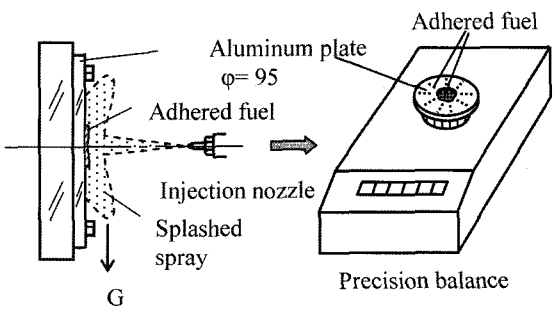

Figure 2. Measurement method of adhered fuel mass.

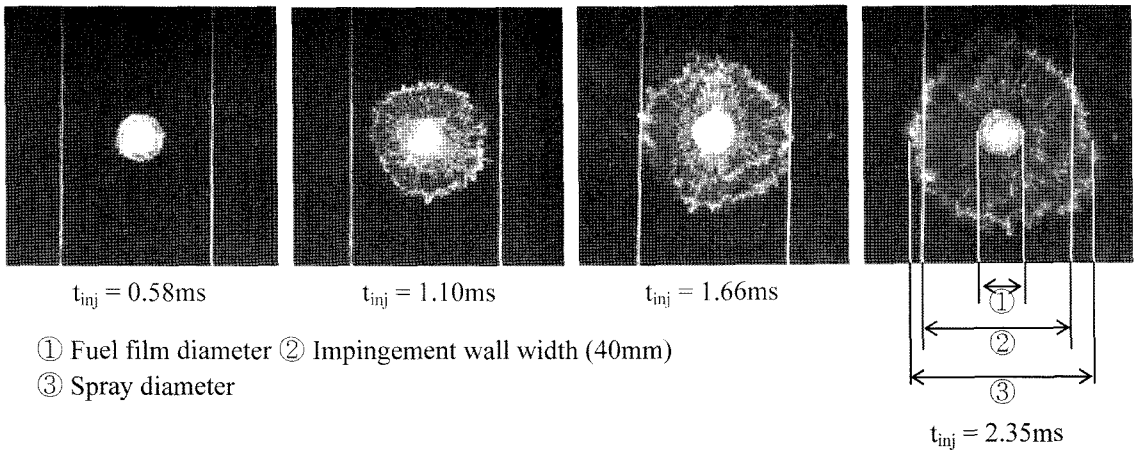

Figure 3. A series of the impinging diesel spray taken from rear view of the transparent wall (L_w=30 mm, P_a=1.5 MPa, τ_w=0.35 ms).

was obtained from total the adhered fuel mass and the surrounding one. In more detail, the total adhered fuel mass, m_{ad} was expressed by;

$$m_{ad} = m_{ad.f} + m_{ad.d}\ , \qquad (1)$$

where, $m_{ad.f}$ is the fuel film mass, and $m_{ad.d}$ is the sparsely adhered fuel droplets encircling the film.

3. EXPERIMENTAL RESULTS

A series of the impinging diesel spray taken from rear view of the transparent wall at wall distance, L_w=30 mm is shown in Figure 3. The impingement time to the wall, τ_w was 0.35 ms after start of injection. On the photograph at the time after start of injection, t_{inj}=0.58 ms, it was observed that a spot of impingement spray and the film of fuel appeared on the wall. However, it was difficult to distinguish the fuel film from the post-impingement spray that was radially spreading on the wall. On the photograph of t_{inj}=1.10 ms, two kinds of spots were observed. One was a clear central spot similar to the spot observed at t_{inj}=0.58 ms and the other was annular image around the central spot. It seemed that the central spot image was corresponding to the wall film and the annular image was the impinged spray spreading on the wall. Then, the fuel film was almost distinguished from post-impingement spray. On the last two photographs, the fuel film was observed clearly enough to be distinguished from post-impingement spray. On the photograph of t_{inj}=2.35 ms, the annular fuel film as well as the post-impingement spray was observed clearly. From the photographs of t_{inj}= 1.10 ms, 1.66 mm and 2.35 ms, it was concluded that the diameter of the fuel film was almost constant, while the diameter of post-impingement spray was developing larger as time elapsed.

For various wall distances and ambient pressures, the maximum fuel film diameter is shown in Figure 4. In this study, the experiment had been conducted 3 times or more for one experimental condition. Three data for one condition were indicated in the figure, and the data error range was less than 3 percent. Because the fuel film diameter had been hardly changed since it became constant, as shown in Figure 3, the value at that time was measured as the maximum fuel film diameter. As the wall distance became longer, the fuel film diameter also became larger, having the value of from 8 mm to 16 mm. As the ambient pressure became lower, the fuel film diameter became larger.

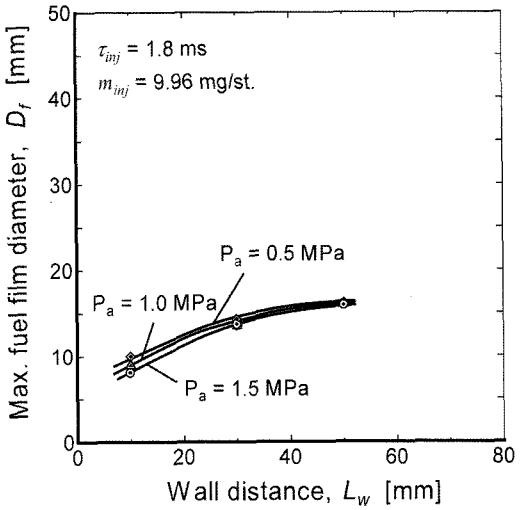

Figure 4. Maximum fuel film diameter for various wall distances and ambient pressures.

To make a detail analysis of adhered fuel, an adhered fuel ratio, α_{ad} was defined as follows.

$$\alpha_{ad} = \frac{\text{adhered fuel mass}}{\text{total injection mass}} \qquad (2)$$

The total injection mass meant the mass of single injection of diesel spray and adhered fuel mass was obtained with the method explained previously. Figure 5 shows adhered fuel ratios under various experimental conditions. In previous study, adhered fuel ratios under injection period of 2.8 ms and total injection quantity of 19.3 mg/st. were obtained, and are expressed as the broken line in the figure (Ko *et al.*, 2001). The adhered fuel ratio of injection period of 2.8 ms was higher than that of 1.8 ms. It seemed that the result was caused by longer injection period than 1.8 ms. Two kinds of adhered fuel ratios were linearly increasing with an increase of impingement wall distance. In the case of L_w=50 m, the mass more than half of injected fuel was adhered on the impingement wall. For both cases, as the ambient pressure increased, the adhered fuel ratio decreased. It might be because as the ambient density becomes higher, droplets become easier to spread into surrounding gas before the droplets arrive on a wall. Since the adhered fuel mass was measured after fuel injection perfectly finished, we could not obtain the adhering fuel ratio with elapsing time. From Figure 4 and Figure 5, both the maximum fuel film diameter and the adhered fuel ratio decreased with an increase of the ambient pressure.

As previously mentioned, mass of sparsely adhered fuel droplets encircling with the fuel film could not be neglected. Then the mass ratio of sparsely adhered fuel droplets to adhered fuel film was calculated and summarized in Figure 6. The ambient pressure was 1.5 MPa. With an increase of the wall distance, the mass ratio of adhered fuel droplets to adhered fuel film decreased. In the case of the wall distance of 10 mm and 30 mm, the mass ratio of adhered fuel droplets to adhered fuel film

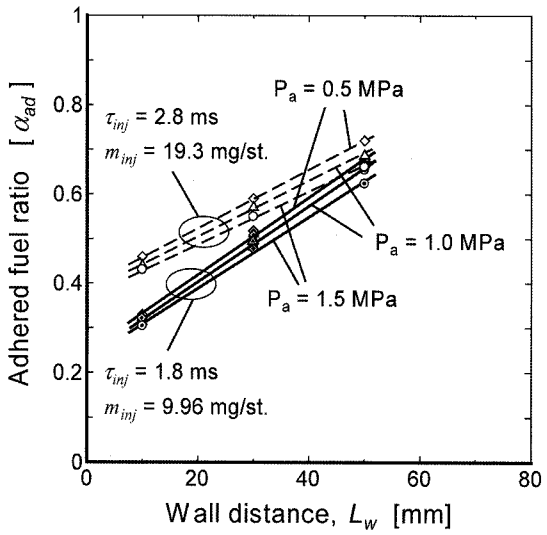

Figure 5. Adhered fuel ratios under various experimental conditions.

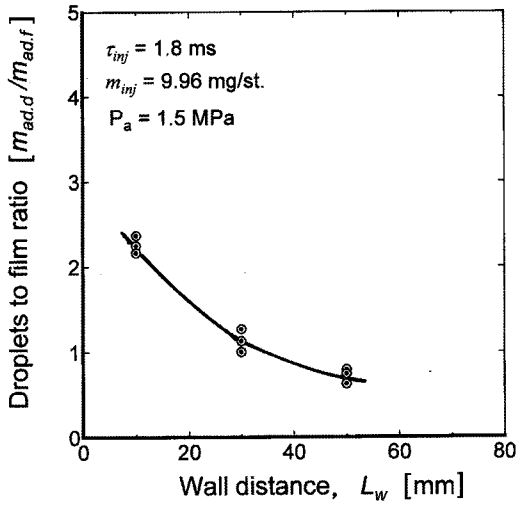

Figure 6. Mass ratios of fuel droplets to fuel film at various wall distances.

exceeded unity. In other words, the fuel droplet more than 50% of the adhered fuel mass was stuck in the vicinity of the fuel film. Although it was not unusual compared with fuel film, these adhered droplets should not be neglected for more precise measurement of adhering fuel mass.

From such photographs as Figure 3, both the spray diameter and the fuel film diameter after wall impingement were obtained under all the experimental conditions. Although the maximum fuel film diameter was obtained, as shown in Figure 4, the fuel film in early stage of the impingement was not easy to distinguish from the post-impingement spray, as shown in the first photograph of Figure 3. That is, the variation of the fuel film diameter in early stage of the impingement could not be clarified because of big experimental uncertainty. Thus it was assumed that the growth of fuel film was a half of that of the post-impingement spray until the film diameter became constant value. This assumption was based on the experiment of Saito *et al.* (1993). Their experiment showed that the radius of the adhered fuel film was about half of the radius of the spray in early stage of the impingement.

Under the above assumption, the spray diameter after impingement and the fuel film diameter with elapsing time are shown in Figure 7. The wall distance was 30 mm and the ambient pressure was 1.5 MPa. The spray impingement occurred at 0.35 ms after start of injection. The spray diameter and the maximum fuel film diameter were obtained by using the drum camera and still camera, respectively. The fuel adhering on the wall could be measured by means of dividing into two zones, film zone and droplets zone, as shown in the figure.

The adhering fuel mass on a wall changes as time progresses. It was impossible to measure directly the

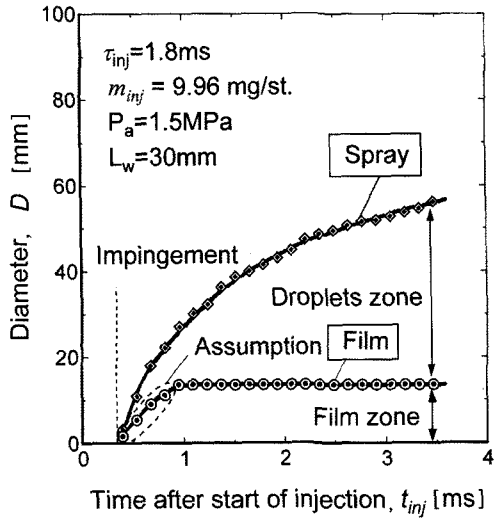

Figure 7. The spray diameter after impingement and the fuel film diameter at various timings.

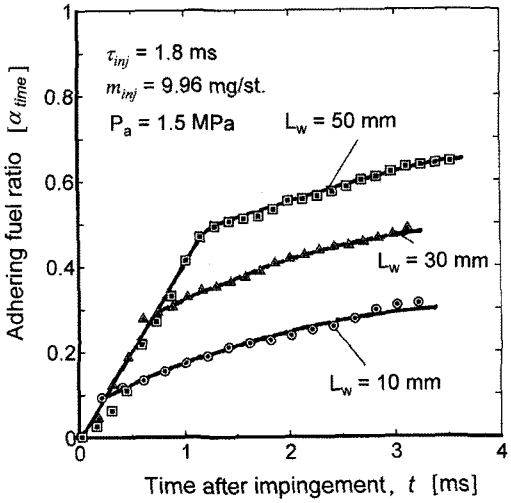

Figure 8. Adhering fuel ratios with elapsing time at various wall distances.

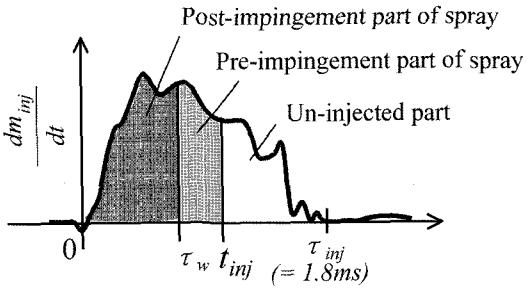

Figure 9. Injection rate diagram.

variation of adhering fuel mass with elapsing time. According to the result of simulation work conducted by Senda *et al.* (1997), the fuel film thickness had a maximum value at the impinging point, and decreased with increase of radial distance. Stanton and Rutland (1996) also reported in their numerical simulation work that the film thickness was not constant during the impingement. However, it was very difficult to obtain reliable results on the film thickness profiles with elapsing time in this experimental study on diesel impingement spray. If the fuel film adheres with the same thickness in film zone and the fuel droplets adhere equally through the droplets zone, the adhering fuel mass can be estimated as a function of time. Based on the assumption including the assumption in Figure 7, the adhering fuel ratio was calculated under the ambient pressure of 1.5 MPa. The adhering fuel ratio, α_{time} was defined as follows.

$$\alpha_{time}=\frac{\text{adhering fuel mass with elapsing time}}{\text{total injection mass}} \quad (3)$$

The results are shown in Figure 8. Adhering fuel ratios increased with elapsing time at all the wall distances. As the spray impingement were progressing on, adhering fuel ratios increased more and more, and finally became about 30%, 50% and 65% for L_w=10 mm, 30 mm and 50 mm conditions, respectively. In the figure, adhering fuel ratios increased steeply in early stage of the impingement, and then increased slowly after around 0.2 ms, 0.7 ms and 1.2 ms from the impingement for L_w=10 mm, 30 mm and 50 mm, respectively. The changing point corresponded the time that growth of the fuel film finished. That is, more fuel was adhered on the wall for a growing period of the fuel film diameter, in comparison with for a constant period of it. The fuel mass from start of injection to a certain time in the injection process was derived from the injection rate diagram shown in Figure 9. Where, dm_{inj}/dt is the injection rate, t_{inj} is time after start of injection, τ_w is the impingement time to the wall, and τ_{inj} (=1.8 ms for the case of L_w=10 mm, 30 mm and 50 mm) is injection period. The un-injected part means the part that is not injected yet.

The distribution of fuel mass was evaluated by dividing into three types according to the spray impingement process. The outline of the evaluation method is explained with Figure 10 as follows.

(1) The fuel mass before spray impingement, that is, the fuel mass m_1 of pre-impingement spray was expressed by;

$$0 \le t_{inj} \le \tau_w$$

$$m_1=\int_0^{t_{inj}} \frac{dm_{inj}}{dt} dt \quad (4)$$

(2) Spray impinging on a wall could be divided into the part before impingement (pre-impingement spray), the part after impingement (post-impingement spray) and the adhering part on the wall. Accordingly, the fuel mass m_1 of pre-impingement spray, the fuel

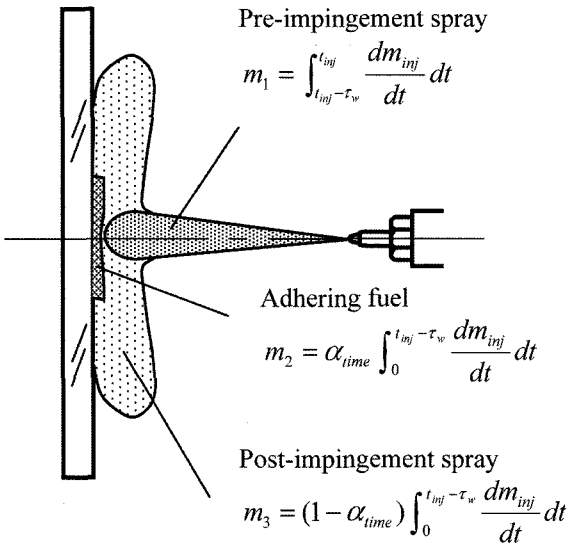

Figure 10. Distribution of injected fuel mass on an impinging spray.

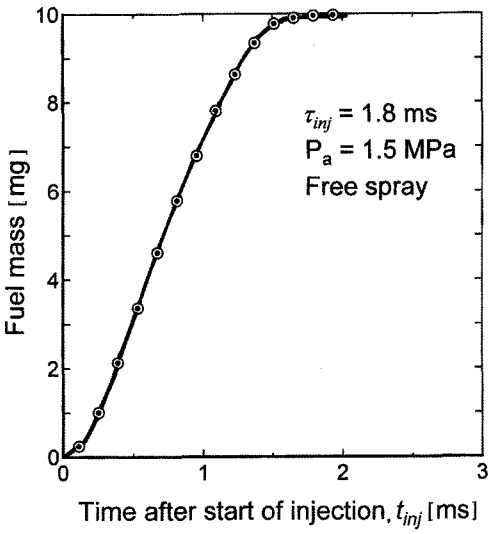

Figure 11. The injected fuel mass of free spray at various timings.

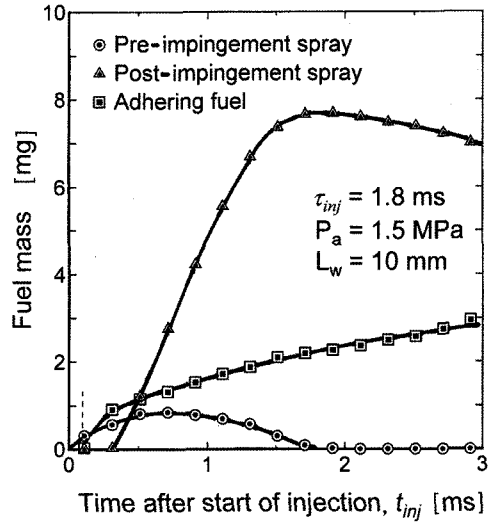

Figure 12. Distribution of fuel mass on spray impinging at L_w=10 mm.

mass m_2 adhering on the wall and the fuel mass m_3 of post-impingement spray are expressed as follows, using the adhering fuel ratio, α_{time}.

$\tau_w < t_{inj} \leq \tau_{inj} + \tau_w$

$$m_1 = \int_{t_{inj}-\tau_w}^{t_{inj}} \frac{dm_{inj}}{dt} dt \quad (5)$$

$$m_2 = \int_0^{t_{inj}-\tau_w} \frac{dm_{inj}}{dt} dt \quad (6)$$

$$m_3 = (1-\alpha_{time}) \int_0^{t_{inj}-\tau_w} \frac{dm_{inj}}{dt} dt \quad (7)$$

(3) When t_{inj} was over $\tau_w + \tau_{inj}$, it was considered that all the injected fuel was impinged on the wall. The fuel mass after impingement process was expressed by;

$\tau_{inj} + \tau_w < t_{inj}$

$$m_1 = 0 \quad (8)$$

$$m_2 = \alpha_{time} \int_0^{t_{inj}} \frac{dm_{inj}}{dt} dt = \alpha_{time} m_{inj} \quad (9)$$

$$m_3 = (1-\alpha_{time}) \int_0^{t_{inj}} \frac{dm_{inj}}{dt} dt = (1-\alpha_{time}) m_{inj} \quad (10)$$

Based on the above equations, the variations of fuel masses under the ambient pressure of 1.5 MPa are given in Figure 11 to Figure 14. Integration of the mass according to elapsing time is shown in Figure 11. A small quantity of fuel was injected up to 0.1 ms after start of injection. After that time, however the fuel mass rapidly increased up to 1.5 ms. And then, the fuel mass increased very slowly up to 1.8 ms of injection end.

As for pre-, post-impingement sprays and fuel adhering on the flat wall set at L_w=10 mm, the distributions of fuel masses are shown in Figure 12. The vertical broken line in the figure corresponds to the impingement time to the wall. The fuel mass of post-impingement spray was twice or more as much as that of adhering fuel, when the time was over 0.7 ms after start of injection. As for the part of pre-impingement spray, however, the fuel mass decreased after 0.7 ms, and finally became zero around 1.9 ms. The fuel mass of adhered part increased rapidly in early stage of the impingement, and then increased comparatively slowly. This change was observed at the time of 0.3 ms when the fuel film diameter approached constant value. On the other hand, the fuel mass of post-

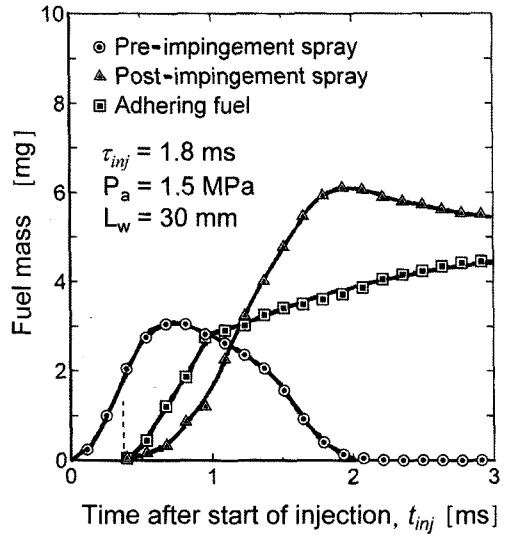

Figure 13. Distribution of fuel mass on spray impinging at L_w=30 mm.

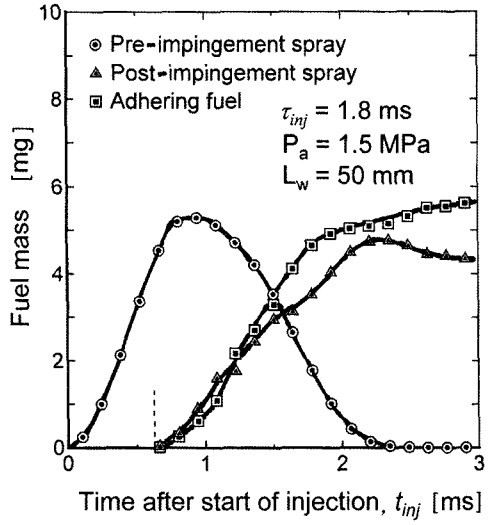

Figure 14. Distribution of fuel mass on spray impinging at L_w=50 mm.

impingement spray began to decrease slowly after passing 1.5 ms. The injection period of the spray was 1.8 ms. However the mass of adhering fuel still increased with elapsing time after injection finished. It was considered that the spray tail motion was becoming slow after the end of injection and it caused the late adhering motion of the spray.

Figure 13 shows the distribution of fuel mass for the spray impinging at L_w=30 mm. The fuel mass of pre-impingement spray increased until around 0.75 ms, and then decreased. With regard to the adhering fuel, the fuel mass increased steeply up to 0.9 ms. Like in Figure 12, it was found that the fuel film diameter had constant value around 0.9 ms. The maximum value for the fuel mass of post-impingement spray occurred around 2.0 ms after start of injection and then the fuel mass decreased slowly.

In the case of L_w=50 mm, three types of fuel mass distribution are shown in Figure 14. The fuel mass of pre-impingement spray steeply increased up to 0.9 ms, and decreased rapidly. The fuel mass of post-impingement spray increased with almost the same way as the adhering fuel until 1.5 ms after start of injection. After then, however, the mass of adhering fuel exceeded that of the post-impingement spray. After 2.2 ms, the mass of post-impingement spray decreased slowly, while the mass of adhering fuel increased slowly.

4. CONCLUSIONS

In order to clarify the characteristics and the effect of adhering fuel, the photograph of fuel film was taken with elapsing time and the adhered fuel mass was measured in detail. Also the distribution of fuel mass for the impinging diesel spray was analyzed as a function of time. The major conclusions are as follows.

(1) Both the maximum fuel film diameter and the adhered fuel ratio decreased with an increase of the ambient pressure.

(2) The mass ratio of adhered fuel to total injection fuel became larger with an increase of the impingement distance. Its value was over the half of the total injection fuel mass at the condition of Lw=50 mm.

(3) It was assumed that the growth of fuel film was a half of that of the post-impingement spray until the film diameter became constant value. Further, if the fuel film adheres with the same thickness in film zone and the fuel droplets adhere equally through the droplets zone, the adhering fuel mass increased rapidly until the fuel film diameter approached maximum value, and then increased comparatively gradually.

(4) Though the spray tail motion was slow, the adhering fuel mass still increased after the injection was finished.

ACKNOWLEDGEMENT–The authors would like to express special thanks for Mr. T. Yamada for carrying out the experimental work.

REFERENCES

Amagai, K., Maruyama, Y., Saito, M. and Arai, M. (2003). Spray-to-spray interaction after wall impingement. *SAE Paper No.* 2003-01-1835.

Chikahisa, T., Hishinuma, Y. and Ushida, H. (2002). Mixing conditions with spray-jet interaction for effective soot reduction in diesel combustion. *Int. J. Automotive Technology* **3, 1**, 17–25.

Gonzalez, D., Gonzalez, M. A., Borman, G. L. and Reitz, R. D. (1991). A study of diesel cold starting using both cycle analysis and multidimensional calculations. *SAE Paper No.* 910180.

Ko, K. N., Momiyama, T. and Arai, M. (2001). Effect of wall impingement on volumes of diesel sprays and their concentrations. *Trans. Japan Society of Mechanical Engineers* **67, 662**, 216–222.

Koo, J. Y. (2003). The effect of injector nozzle geometry and operating pressure condition on the transient fuel spray behavior. *J. Mechanical Science and Technology* **17, 3**, 617–625.

Matsuoka, S., Kamimoto, T. and Kobayashi, H. (1984). Photographic and image analysis studies of diesel spray and flame with a rapid compression machine and a D. I. diesel engine (Interpretation and Conceptual Image). *SAE Paper No.* 845009, 76–87.

Park, S. W. and Lee, C. S. (2003). Macroscopic structure and atomization characteristics of high-speed diesel spray. *Int. J. Automotive Technology* **4, 4**, 157–164.

Saito, A., Kawamura, K., Watanabe, S., Takahashi, T. and Tuzuki, N. (1993). Analysis of impinging spray characteristics under high-Pressure fuel injection (1st report, measurement of impinging spray Characteristics). *Trans. Japan Society of Mechanical Engineers* **59, 566**, 356–361.

Senda, J. Kanda, T., Al-Roub, M., Farrell, P. V., Fukami, T. and Fujimoto, H. (1997). Modeling spray impingement considering fuel film formation on the wall. *SAE Paper No.* 970047, 37–51.

Stanton, D. W. and Rutland, C. J. (1996). Modeling fuel film formation and wall interaction in diesel engines. *SAE Paper No.* 960628, 29–45.

Stanton, D. W. and Rutland, C. J. (1998). Multi-dimensional modeling of thin liquid films and spray-wall interactions resulting from impinging sprays. *Heat and Mass Transfer,* **41**, 3037–3054.

Takasaki, K., Wakuri, Y., Maeda, K., Oyamada, T. and Hamasaki, K. (1994). Influence of fuel spray impingement on combustion in a D. I. diesel engine. *The 3th Int. Sym. Diagnostics and Modeling of Combustion in Internal Combustion Engines*, July 11–14, Yokohama, Japan, 269–274.

Tsunemoto, H., Ishitani H., Wakamatsu T. and Tanaka T. (1996). Process of mixture formation of impinging spray on the wall in a hole type nozzle. *Trans. Japan Society of Mechanical Engineers* **27, 2**, 39–45.

Zurlo, J. R. and Chigier, N. (1991). Impinging diesel spray dynamics. *Atomization and Sprays,* **1**, 303–318.